DEVELOPMENT OF THE TECHNOLOGY AND EQUIPMENT FOR LASER AND LASER-ARC WELDING OF ALUMINIUM ALLOYS*

G.A. TURICHIN, I.A. TSYBULSKY, E.V. ZEMLYAKOV, E.A. VALDAJTSEVA and **M.V. KUZNETSOV**
St.-Petersburg State Polytechnic University, St.-Petersburg, Russian Federation

Results of computer modelling of the process of hybrid welding of Al–Mg system aluminium alloys up to 10 mm thick by using a dynamic model are considered. Examples of computation of the welding process parameters and their experimental validation are given. The developed technological laser-arc system for implementation of the hybrid welding process is described.

Keywords: *laser and laser-arc welding, aluminium-magnesium alloys, process modelling, computations, geometric characteristics of the weld, thermal cycles, distribution of alloying elements, package of equipment, monitoring of the welding process*

High energy concentration of laser radiation predetermines considerable intensification of the processes of treatment of materials. The concentrated energy input allows materials to be treated at higher speeds and lower residual thermal distortions. Recent achievements in the field of physics and engineering have made it possible to develop new laser radiation sources with much higher energy efficiency.

In welding of alloys, especially light ones based on aluminium, computation of parameters of a welded joint and prediction of its chemical composition and mechanical properties present a difficult problem because of the necessity to allow for removal of volatile additions, such as magnesium, lithium or zinc, which are crucial for the entire set of mechanical properties. Part of these additions is evaporated during welding. As a result, chemical composition and mechanical properties of the weld metal may differ from those of the base metal.

The Al–Mg system is one of the most promising in terms of development of alloys to be welded. Mechanical properties of the welded joints, as well as properties of the base metal, depend mostly on the magnesium content of an alloy, as strength of the alloy grows with increase of the magnesium content. Lithium also exerts a significant effect on properties of aluminium alloys, as variations in the lithium concentration influence both mechanical properties of the alloys and their sensitivity to cracking.

Computer model of laser-arc welding (LAW) based on technologically applicable descriptions of the processes taking place during LAW was used to increase efficiency of development of the LAW technology and equipment [1].

One of the results of many years' efforts is software LaserCad developed by the Institute of Laser and Welding Technologies of the St.-Petersburg State Polytechnic University for modelling of laser, arc and hybrid welding. The software allows computation of geometric characteristics of the weld, thermal cycles in the weld metal and HAZ, and content of alloying elements in the weld metal.

Mathematical modelling of hybrid welding based on the physically adequate model, allowing investigation of relationship between various physical phenomena responsible for development of instabilities in the weld pool, is the most expedient method to analyse causes of the humping effect occurring in the welding process and choose the ways of its elimination. The processes of hybrid LAW with deep penetration, as well as the related processes of laser welding, are often accompanied by formation of porosity and root peaks in the welds [2]. According to current notions about a physical nature of the laser welding processes, this is caused by development of self-oscillations of the keyhole and weld pool in welding with deep penetration [3].

Numerous experimental results confirm that the welding process with deep penetration is not stationary even in the case of stabilisation of all external factors affecting the weld pool [4]. In particular, high-speed filming of laser welding of composite specimens made from metals and optically transparent materials [5] showed a continual variation in shape of the keyhole, quasiperiodic motion of the zone with a maximal intensity in depth of the keyhole, as well as presence of such zones on the rear wall of the keyhole. Filming of the plasma plume also showed the presence of its periodic fluctuations [6].

Comparative investigations of motion of molten metal on the weld pool surface and process of formation of the root peaks confirm correlation between

*Based on the paper presented at the 5th International Conference «Laser Technologies in Welding and Materials Processing (Katsiveli, Ukraine, 24–27 May 2011).

Figure 1. Optical unit of the «Registrator» system (*a*), high-speed digital camera CENTURIO C100 (*b*) and lens spectrograph SL100M (*c*)

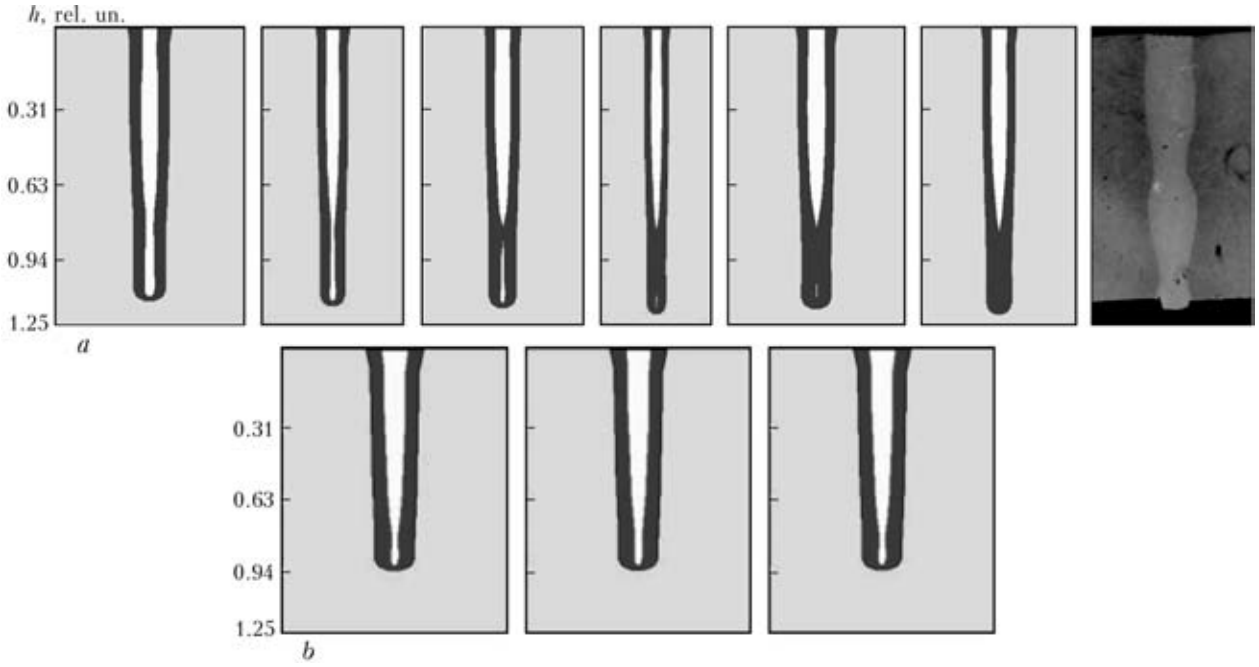

Figure 2. Calculated penetration shapes at v_w = 10 cm/s: *a* — every 1 ms, N = 15 kW; *b* — every 3 ms, N = 12 kW

formation of the peaks and splashing of the molten metal from the weld pool. The same results were obtained later in X-ray filming [7].

The experiments were carried out by using the hybrid LAW system developed and assembled by the Institute of Laser and Welding Technologies of the St.-Petersburg State Polytechnic University. Ytterbium fibre laser LC-15 with a maximal output power of 15 kW was used as a laser radiation source. Radiation was transported via the fibre cable to an optical welding head of the laser-arc module. The «Precitec» welding head YW50 ZK with a focal distance of 400 mm and focal diameter of 0.4 mm, equipped with one-coordinate DC-Scanner having a maximal frequency of 600 Hz and amplitude of up to 10 mm, was used to focus the radiation. Also, the experimental system was fitted with arc power supplies VDU-1500DS and EWM Phoenix 520 RC PULS. Filler metal was fed by using wire feed mechanisms PDGO-511 and Phoenix Drive 4 ROB 2.

Flat specimens measuring 100 × 50 mm, made from alloy AMg6 10 mm thick, and alloy 1424 (Al + + 4.5 % Mg + 1.7 % Li + 0.6 % Zn) 4 mm thick, were penetrated and butt welded during the experiments. Welding was performed with the straight-line welds in flat position. Argon and a mixture of argon with helium were employed to shield the weld pool and weld metal, and wire AlMg6Zr was used as a filler metal.

Quality of all the welds was assessed visually from their appearance and on the base of metallographic examinations of transverse sections. Penetration depth

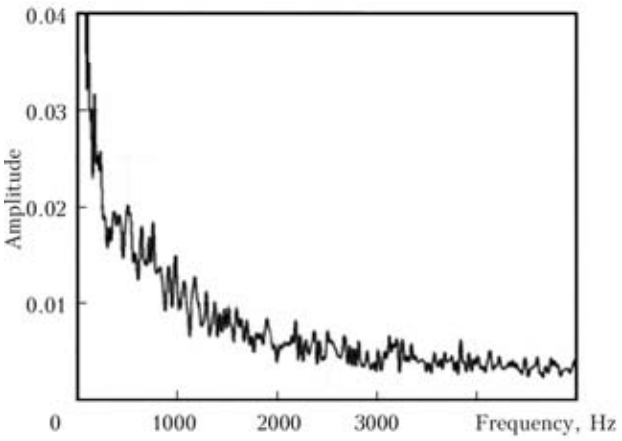

Figure 3. Frequency spectrum of oscillations of the melt

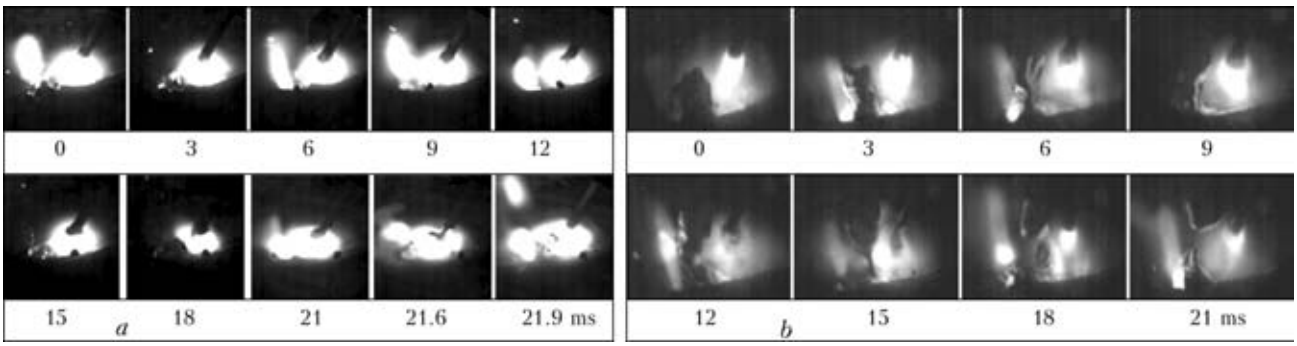

Figure 4. Frames of video filming of the process of formation and detachment of a droplet during hybrid welding using arc power supplies EWM Phoenix 520 RC PULS (*a*) and VDU-1500DC (*b*) at N = 15 kW, v_w = 6 m/min and I_w = 120 A

and other parameters of the weld geometry were determined.

Time characteristics of the dynamic processes occurring in the zone of a hybrid discharge over the workpiece surface were determined by using the plasma plume registration system (Figure 1), which consisted of an optical registration unit with an objective lens, holder for light filter and CCD matrix for registration of signals, and video camera CENTURIO C100 allowing filming at a speed of up to

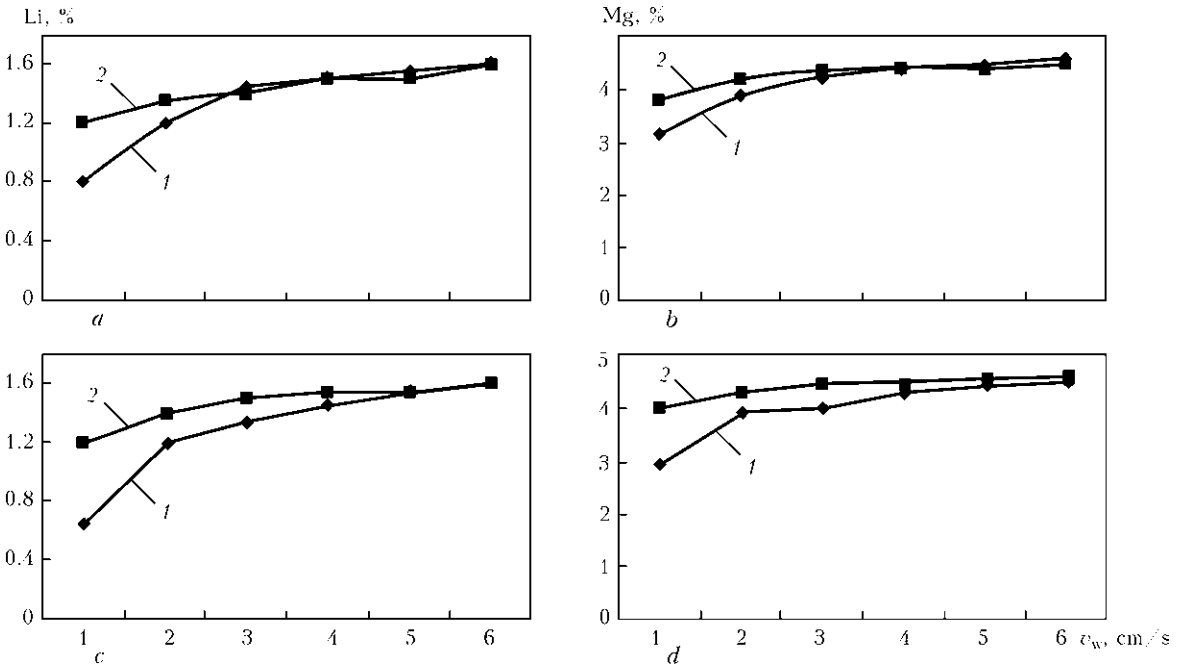

Figure 5. Computed content of lithium (*a*, *c*) and magnesium (*b*, *d*) in the weld metal on a specimen surface in laser welding of alloy 1424 at N = 3500 (*a*, *b*, *d*) and 3000 (*c*) W, d = 0.3 mm and thicknesses of 4 (*1*) and 10 (*2*) mm

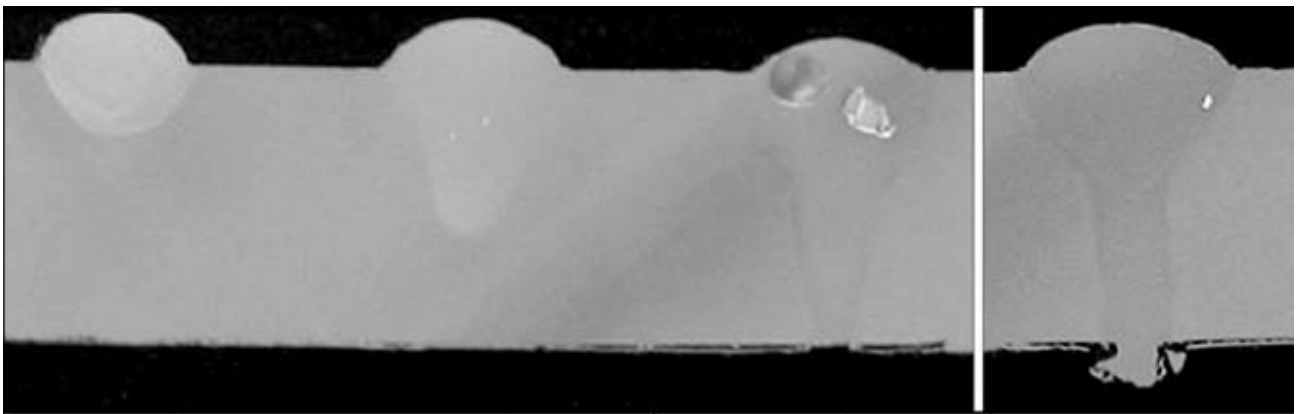

q, J/mm	125	250	300	375
h, mm	3	6	10	10

Figure 6. Results of laser penetration of the AMg6 plate by using filler wire with $v_{f.w}$ = 19 m/min

100,000 frame/s. Lens spectrograph SL100M with astigmatism correction was applied to investigate the optical emission spectrum of the plasma plume.

The computer modelling results obtained with the help of the dynamic model (Figure 2) show that, despite stabilisation of all technological parameters, the process of high-speed welding of thick metals is substantially non-stationary, the root part of the keyhole and penetration channel being most unstable. Characteristic narrowing of the weld, which may lead to formation of a defect, can be seen in Figure 2, *a*, which shows cross sections of the laser weld made at the

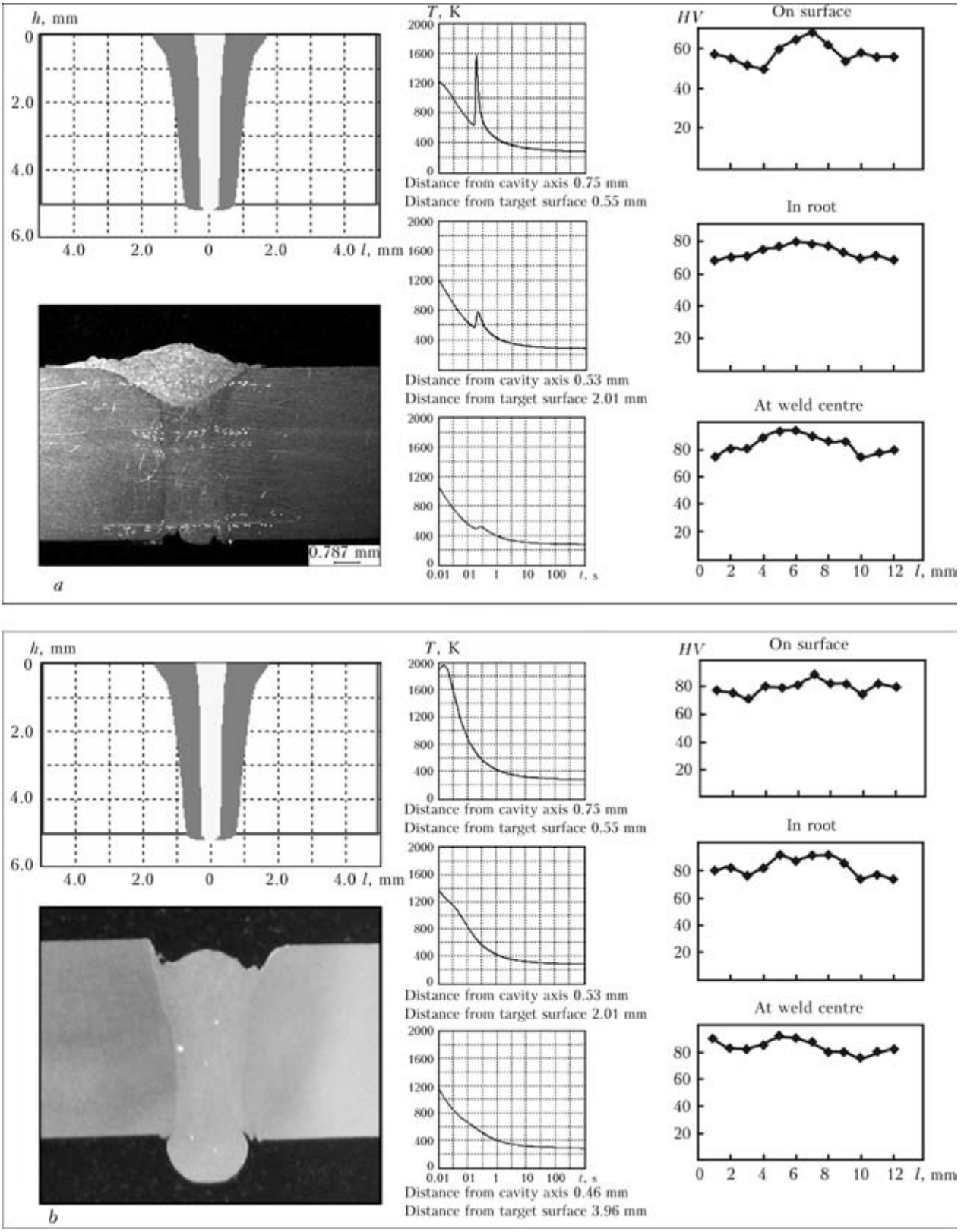

Figure 7. Computation data on shape of cross section, thermal cycles of the weld and microhardness after laser-arc welding of aluminium alloy (q = 100 J/mm): *a*, *b* — distance between laser beam and electrode equal to 15 and 2 mm, respectively

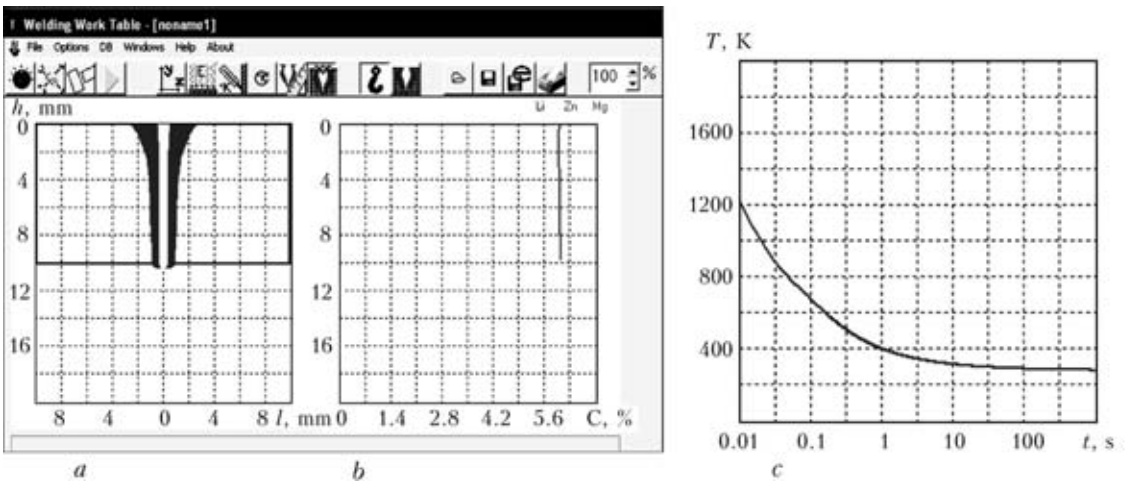

Figure 8. Computed cross section of the penetration zone (*a*), distribution of magnesium in depth of the weld (*b*), and thermal cycle in hybrid welding of alloy AMg6 (*c*)

same process parameters with an interval of 1 ms. A more stable weld pool can be provided by using circular scanning of the laser beam with small (up to 0.5 mm) radii and high (above 300 Hz) frequency of scanning (Figure 2, *b*). The absence of this stabilisation may lead to formation of large-diameter pores and root peaks, resulting from collapse of the keyhole.

The experiments showed that dynamic behaviour of brightness of radiation of the melt is characterised by the presence of low-frequency oscillations. These frequencies were determined by means of computer modelling using the dynamic model, as well as experimentally by means of photodiodes directed to the weld pool. Figure 3 shows the characteristic frequency spectrum of signals from the photodiodes.

The speed of video filming is determined by the frequency of oscillations of the melt. Analysis of dynamic behaviour of the melt pool showed the absence of oscillations with frequencies of over 500 Hz in the melt. Therefore, to examine the surface of the weld pool the speed of filming should be not less than 1000 frame/s (Figure 4).

Analysis of the high-speed filming frames allowed determination of position of an electrode relative to the laser beam.

Results of computation of the amount of alloying elements made with software LaserCAD at different thicknesses and process parameters for alloy 1424 are shown in Figure 5. Decrease in the welding speed leads to increase in losses of volatile alloying elements that provide high service properties of alloys, this leading to weakening of the weld.

Due to evaporation, the content of impurities in the weld metal in welding at decreased speeds is substantially different from that in the base metal, especially in the upper part of the molten zone, where radius of the keyhole is maximal. As the upper part of the keyhole is of a decisive character for the process of multiple re-reflections in this keyhole, evaporation of impurities considerably changes the shape and size of the penetration zone. An example of such broadening is shown in Figure 6. Increase of heat input in laser welding using filler metal led to a substantial growth of the penetration zone.

In addition to the high-speed video filming, thermal cycles were computed and microhardness in the laser-affected zone (Figure 7) was measured to determine position of the electrode relative to the laser beam.

Structure of the weld metal across its section in hybrid welding is homogeneous, consisting of fine dendrites. In case of an increased distance between the heat sources, the time of dwelling of the weld metal at increased temperatures is longer and, as a result,

	LW	LAW + MIG	LW + MIG
Investigation object			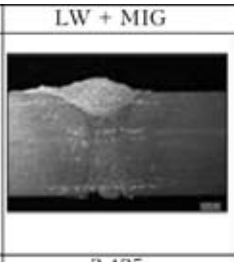
On surface	5.298	6.485	3.135
In root	4.624	5.871	3.274
At centre	5.710	5.510	3.279
Base metal	6.442		2.648
Welding wire		6.25	

Figure 9. Distribution of the amount of magnesium in depth of the weld in different method of welding of aluminium alloy

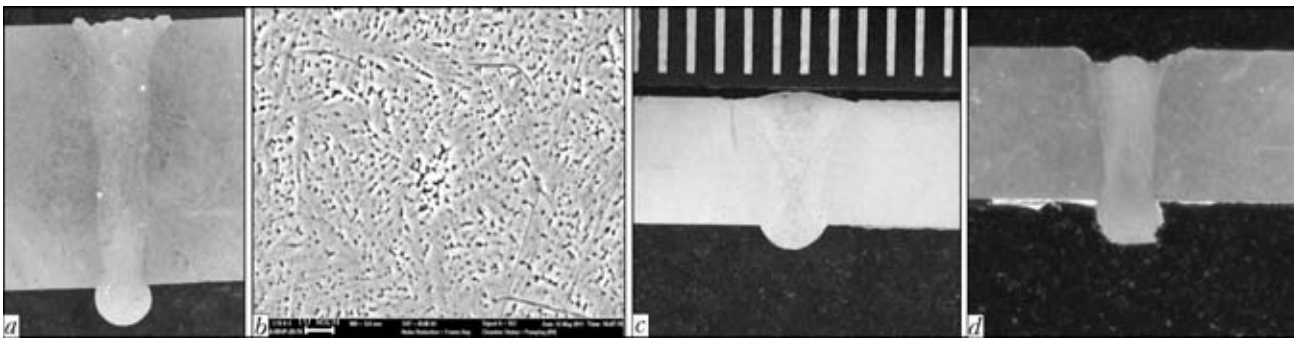

Figure 10. Cross sections of the welds in LAW of alloys AMg6 (*a*), 1424 (*c*) and Al–Mg3 (*d*), and microstructure of the weld metal on alloy AMg6 (*b*)

the dendrites in the upper part of the weld increase in size. In the hybrid process, microhardness of the weld metal is close to that of the base metal, this being caused both by its fine-dendritic structure and higher magnesium content.

Further experiments were carried out at the maximal welding speed and a distance between the laser beam and electrode equal to 2 mm.

An example of modelling of hybrid welding of alloy AMg6 is shown in Figure 8.

The X-ray spectrum microanalysis results shown in Figure 9 confirmed the computed values. As seen from this Figure, the use of filler metal allows compensation for the losses of alloying elements.

Figure 10 shows a cross section and microstructure of metal of the butt weld with through penetration of the 10 mm thick plates of alloy AMg6 (q = = 175 J/mm) and, as examples of welding of other alloys, cross sections of the welds on the 5 mm thick plates of alloys 1424 and Al–Mg (q = 100 J/mm).

The laser-arc technological system (LATS) was developed and manufactured in the course of the work. It consists (Figure 11) of a laser unit (fibre laser), arc equipment package, laser-arc module (work tool), manipulator, gas preparation and distribution unit, seam monitoring subsystem (seam guidance), process monitoring subsystem, and automatic control system. LATS is equipped with a system for guiding the laser-arc module to the joint welded, which is based on a triangulation laser sensor. This system provides monitoring of geometric parameters of a welded joint and tracking the coordinates of the joints at a welding speed of up to 6 m/min with the following parameters: ±0.5 mm in a transverse direction relative to the joint, and ±0.2 mm in the vertical direction.

The investigation results on dynamics of behaviour of the weld pool and vapour-plasma plume allowed the development of equipment for control of the technological process integrated into the welding process monitoring system.

CONCLUSIONS

1. The possibility was shown of using scanning to improve the quality of the welds.

Figure 11. General view of LATS

2. The required frequencies of scanning corresponding to fluctuations of the weld pool were determined.

3. It was shown that the character of penetration and properties of the weld metal depend on the laser beam–arc distance.

4. It was shown that the content of alloying elements in the weld metal decreases with increase of the welding speed.

5. It was confirmed that filler metal compensates for the losses of alloying elements in LAW.

6. Welded joints characterised by a high depth to width ratio, high quality and low distortions were produced on aluminium-base alloys.

1. Turichin, G. (1997) Model of laser welding for technology application. In: *Proc. of the Academy of Sci., Physics Series*, 61(**8**), 1613–1618.
2. Matsunawa, A., Mizutani, M., Katayama, S. et al. (2003) Porosity formation mechanism and its prevention in laser welding. *Welding Int.*, 17(**6**), 431–437.
3. Lopota, V., Turichin, G., Tzibulsky, I. et al. (1999) Theoretical description of the dynamic phenomena in laser welding with deep penetration. In: *Proc. of SPIE*, Series 3688, 98–107.
4. Forsman, T., Powell, J., Magnusson, C. (2001) Process instability in laser welding of aluminium alloys at the boundary of complete penetration. *J. Laser Appl.*, 13(**10**), 193–198.
5. Bashenko, V.V., Mitkevich, E.A., Lopota, V.A. (1983) Peculiarities of heat and mass transfer in welding using high energy density power sources. In: *Proc. of 3rd Int. Coll. on EBW* (Lion, 1983), 61–70.
6. Lopota, V.A., Smirnov, V.S. (1989) Structure of material and its parameters in beam-affected zone in laser welding with deep penetration. *Fizika i Khimiya Obrab. Materialov*, **2**, 104–115.
7. Matsunawa, A., Kim, J.-D., Seto, N. et al. (1998) Dynamics of the keyhole and molten pool in laser welding. *J. Laser Appl.*, 10(**12**), 247–254.